Supplementary Information

Hwang *et al.*

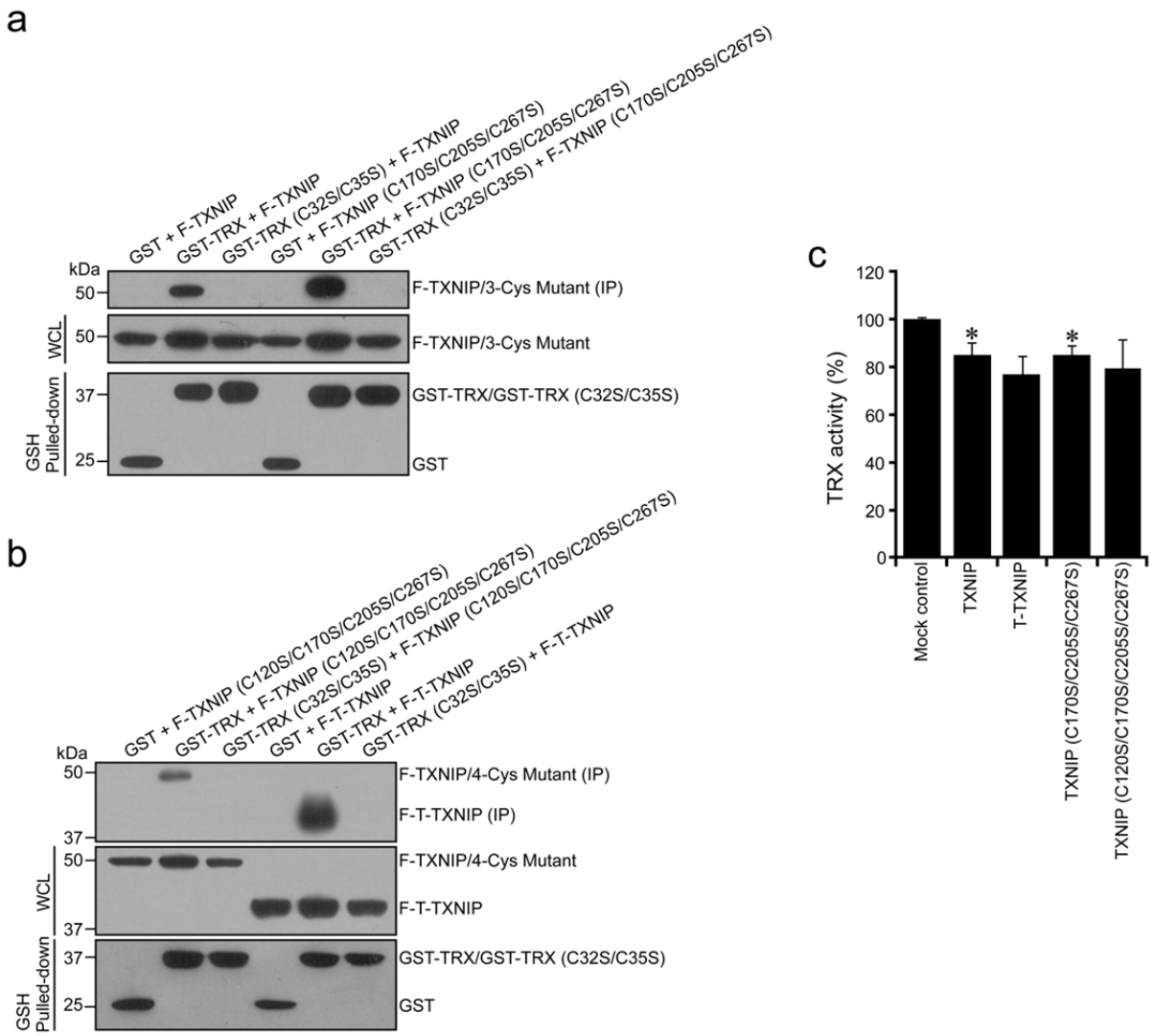

Supplementary Figure S1 | The abilities of the TXNIP mutants and T-TXNIP to bind to and negatively regulate TRX are equivalent to that of native TXNIP. (**a**,**b**) HEK 293T cells were transfected with the indicated plasmids. The cells were lysed and then GST and GST-fusion proteins were pulled down with glutathione beads and immunoblotted with anti-FLAG (F) or anti-GST antibodies. One percent of each whole cell lysate (WCL) was used as

the input. The 3-Cys and 4-Cys mutants indicate the F-TXNIP(C170S/C205S/C267S) and F-TXNIP(C120S/C170S/C205S/C267S), respectively. The data are representative of two independent experiments. (**c**) The inhibiting activities of TXNIP and its variants towards endogenous TRX were detected using an insulin disulfide reduction assay. The data are represented as a percentage of the activity of mock-transfected cells and are shown as the mean ± S.D. of n = 3 independent experiments. **P* < 0.05, compared with mock transfection (Student's *t*-test).

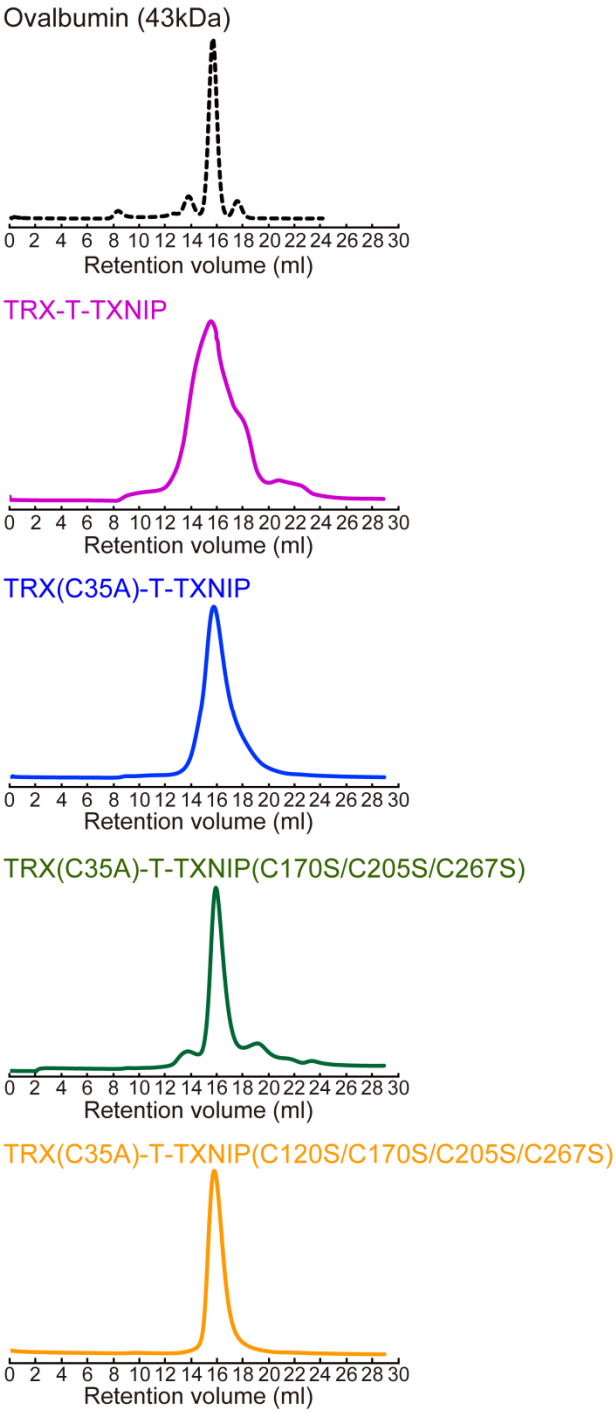

Supplementary Figure S2 | The TRX-T-TXNIP complex exists as a single heterodimer in solution. Size-exclusion chromatography analysis of the wild-type TRX-T-TXNIP complex and its variants. Ovalbumin was used as a size marker.

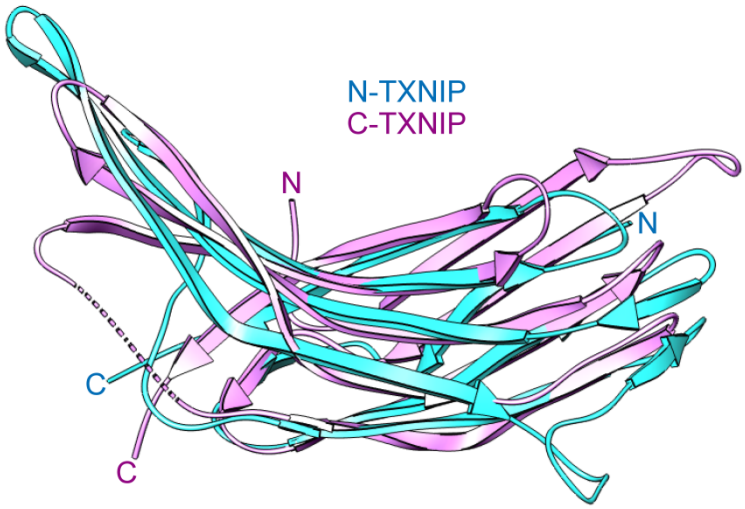

Supplementary Figure S3 | Structural analysis of T-TXNIP domains. The C-TXNIP structure (magenta) is superimposed onto the N-TXNIP structure (cyan).

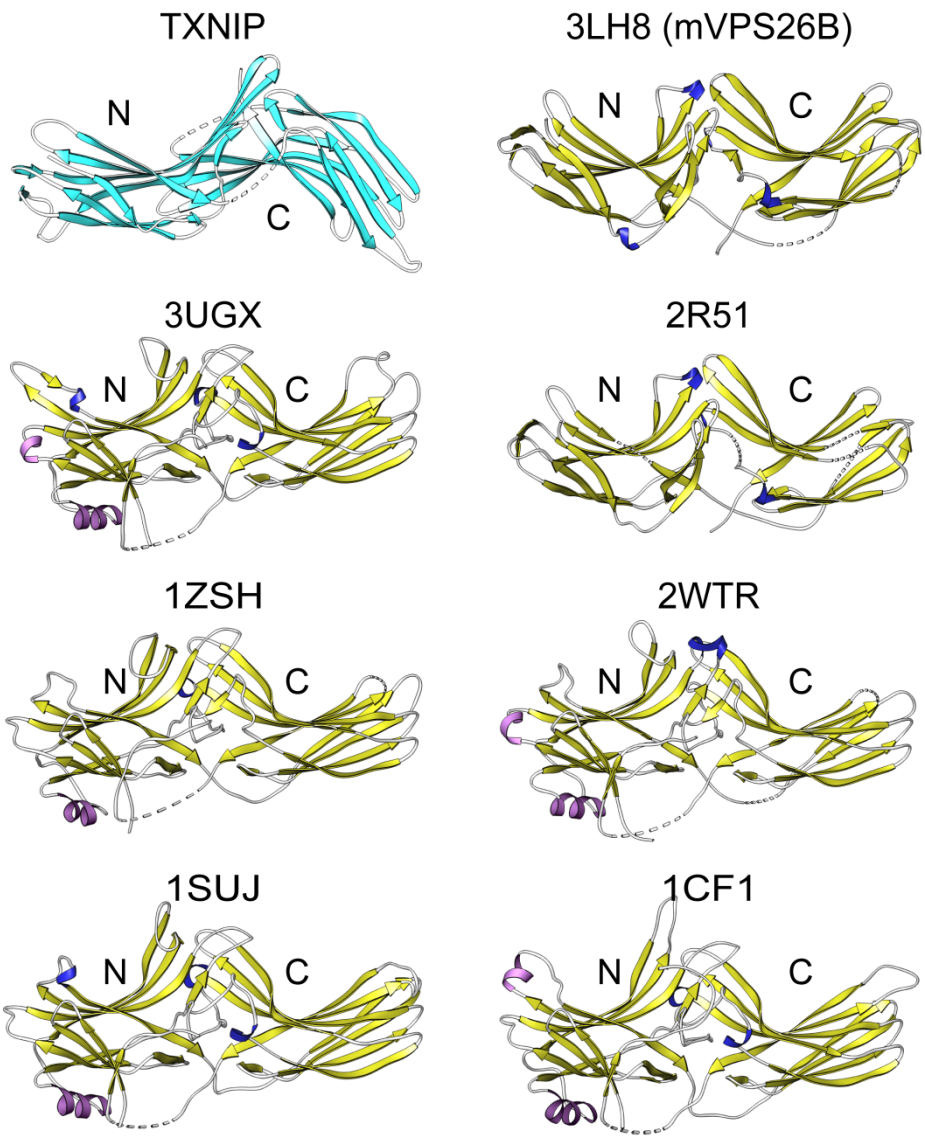

Supplementary Figure S4 | The domain assemblies of TXNIP and other arrestin family proteins. The folding of TRX-bound TXNIP differs from all previously reported arrestin family proteins. The PDB accession IDs of the representative arrestin structures used are shown. The N-terminal and C-terminal domains of each structure are indicated.

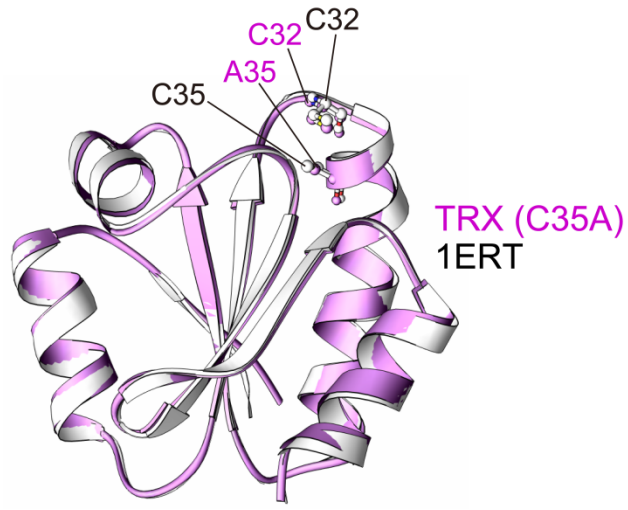

Supplementary Figure S5 | Structural comparison of T-TXNIP-bound and free TRX. No significant structural differences were observed between TRX (C35A) complexed with T-TXNIP (magenta) and free TRX (PDB accession ID: 1ERT) (white). The residues at positions 32 and 35 are indicated.

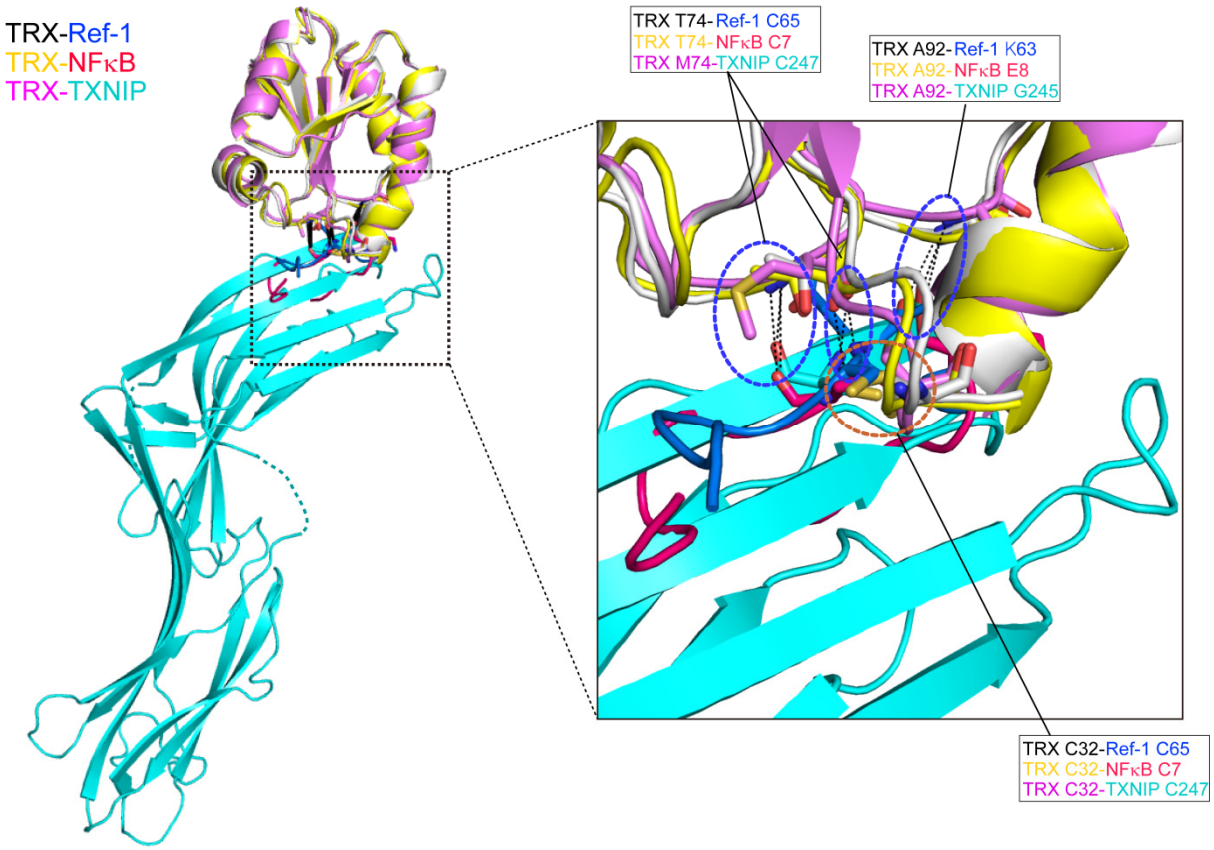

Supplementary Figure S6 | Superimposition of TRX-interacting substrates. Structures of the TRX-Ref-1 (PDB accession ID: 1CQG) (white-blue), TRX-NF-κB (PDB accession ID: 1MDI) (yellow-red), and TRX-TXNIP (magenta-cyan) complexes. The consensus backbone-backbone interactions stabilizing intermolecular disulfides in each complex are highlighted by dashed blue circles and the residues involved in the interactions are indicated. The cysteine residues involved in the intermolecular disulfide formation in each complex are indicated by the dashed brown circle.

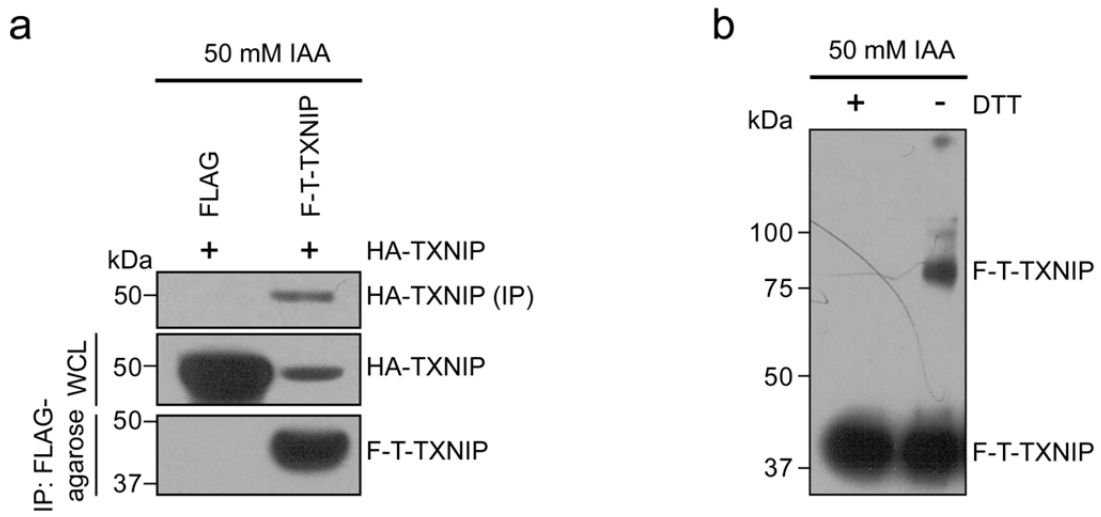

Supplementary Figure S7 | The interprotomer interaction between TXNIP molecules *in vivo*. Immunoprecipitation assays were performed using lysates from 293T cells transfected with FLAG-tagged (F) and HA-tagged TXNIP. The cells were disrupted in lysis buffer containing 50 mM iodoacetamide (IAA). (**a**) Immobilized proteins on FLAG-agarose beads were visualized by immunoblotting using anti-FLAG or anti-HA antibodies. (**b**) Immobilized proteins on FLAG-agarose beads were fractionated by SDS-PAGE under reducing (+ DTT) and non-reducing (- DTT) conditions and visualized by immunoblottng using an anti-FLAG antibody. The data are representative of two independent experiments.

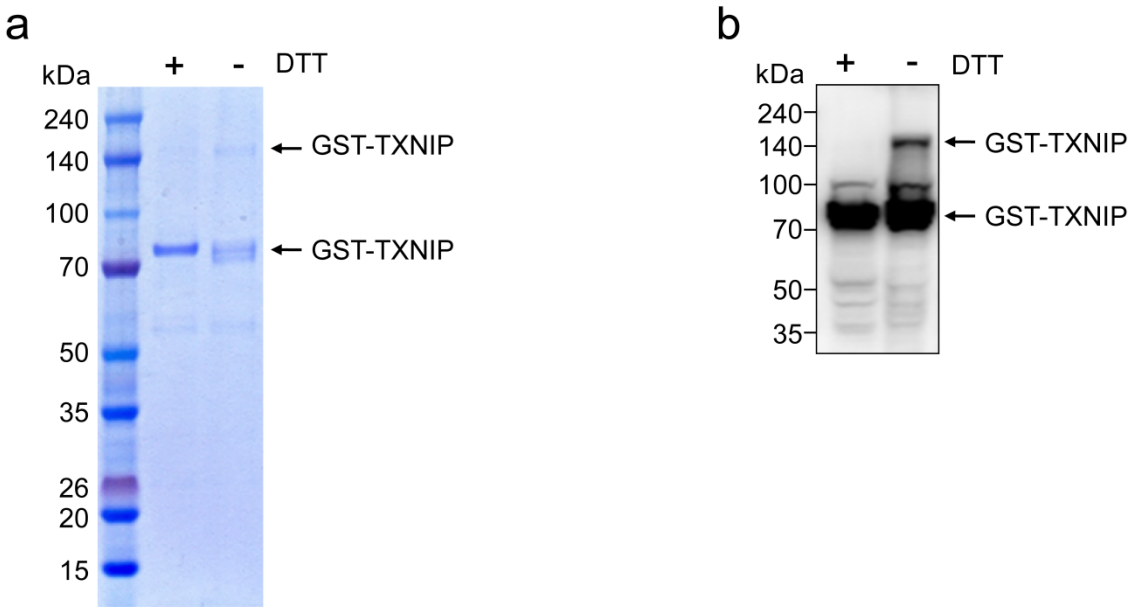

Supplementary Figure S8 | TXNIP molecules interact with each other in a redox-dependent manner. Pull-down assays were performed using lysates from 293T cells transfected with a plasmid expressing GST-fused TXNIP. Immobilized proteins on glutathione beads were fractionated by SDS-PAGE (**a**) and analyzed by immunoblotting using an anti-GST antibody (**b**). Similar results were obtained in two independent experiments.

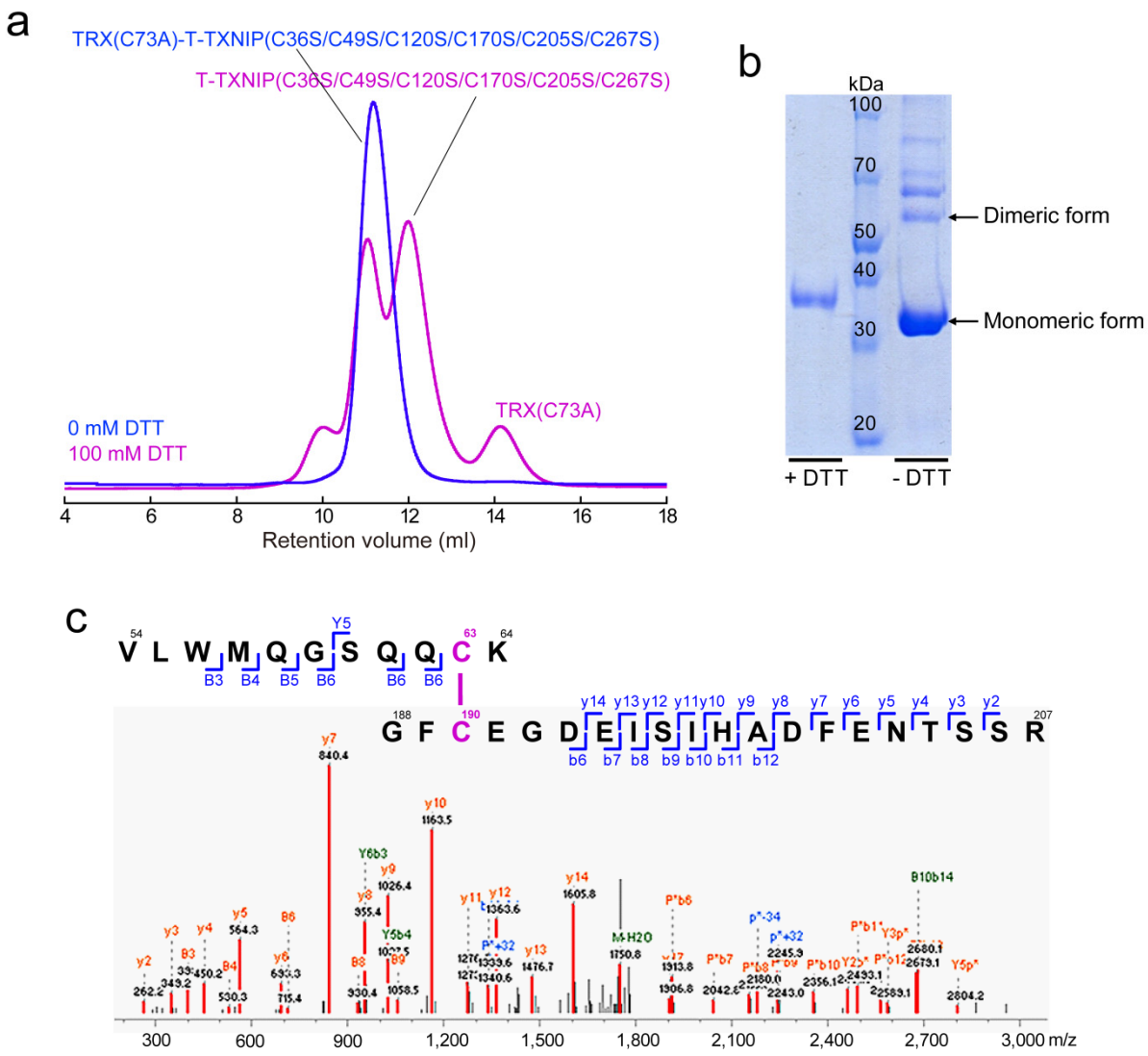

Supplementary Figure S9 | Proteomic analysis of TXNIP. (**a**) Size-exclusion chromatography analyses of the purified TRX(C73A)-T-TXNIP(C36S/C49S/C120S/C170S/C205S/C267S) complex incubated without (blue) or with (magenta) 100 mM DTT to separate T-TXNIP(C36S/C49S/C120S/C170S/C205S/C267S) and TRX. The fractions containing T-TXNIP(C36S/C49S/C120S/C170S/C205S/C267S) were collected and dialyzed against 50 mM Tris-HCl (pH 8.0), 500 mM NaCl, and 10% glycerol to induce the formation of disulfide bonds between TXNIP molecules. (**b**) SDS-PAGE analysis of the interprotomer-interacting TXNIP molecules. Reducing and non-

reducing protein samples were fractionated by SDS-PAGE. The bands at approximately 32 kDa and 60 kDa represent monomeric and dimeric T-TXNIP(C36S/C49S/C120S/C170S/C205S/C267S), respectively. These two protein bands were subjected to a disulfide bond proteomic analysis. The remainders of the high molecular bands were analyzed as non-specific aggregates of TXNIP molecules. No disulfide bonds were detected in the bands. (**c**) MS/MS spectrum of the interdomain disulfide bond between Cys63 and Cys190 in the 32 kDa band, identified as ^{54}VLWMQGSQQ<u>C</u>K^{64}-^{188}GF<u>C</u>EGDEISIHADFENTSSR^{207}. Doubly-charged $[M+2H]^{+}$ peptide ions at m/z 1759.77 were fragmented via higher-energy collisional dissociation. The standard backbone fragments that occurred by amide bond cleavages were highly abundant. The persulfide ion (p+32) and dehydroalanine ion (p-34) formed by C-S bond cleavage reactions were also identified. Matched peaks are shown in red. The ion types of matched peaks are written in red for b- and y-ions, blue for ions from C-S and S-S bond cleavages, and green for disulfide bond-linked internal ions. Annotations used are: P, strand VLWMQGSQQCK; p, strand GFCEGDEISIHADFENTSSR; B and Y, ions from P; b and y, ions from p; P+32, persulfide ion of P; p-34, dehydroalanine ion of p.

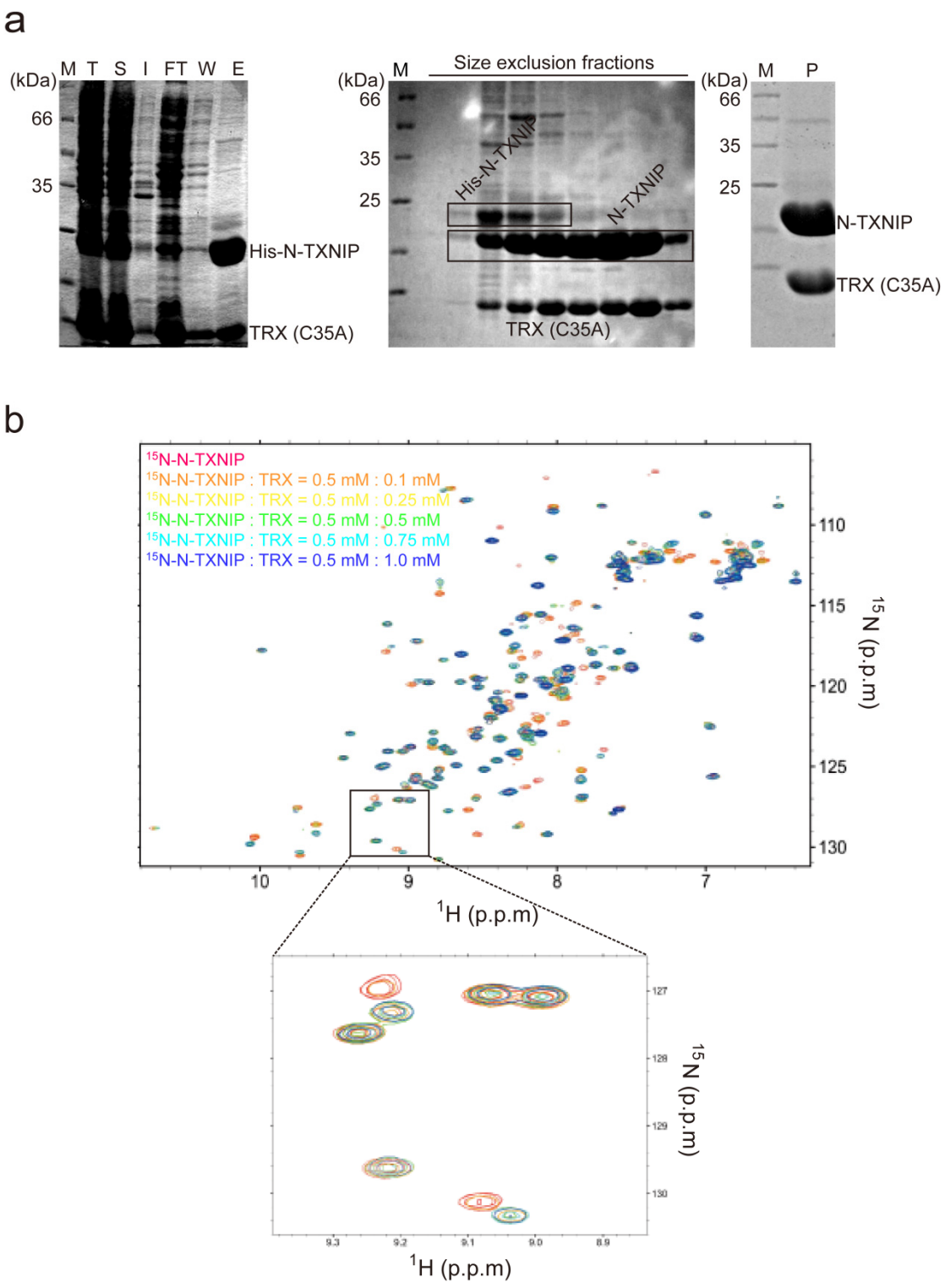

Supplementary Figure S10 | N-TXNIP interacts with TRX. (**a**) SDS-PAGE analysis of N-TXNIP co-expressed and co-purified with TRX(C35A). M, molecular weight size marker; T, total cell lysate; S, soluble fraction; I, insoluble fraction; FT, flow-through fraction; W, wash

fraction; E, hexahistidine-tagged N-TXNIP eluted from the Ni-NTA column; N-TXNIP, tag-free N-TXNIP obtained by treatment with recombinant TEV protease; P, purified protein. (**b**) Representative ^{15}N-HSQC NMR spectra of N-TXNIP after the addition of increasing amounts of TRX. The inset shows the chemical shift perturbations that occurred upon the addition of 0 (red), 0.2 (orange), 0.5 (yellow), 1 (green), 1.5 (cyan), and 2 (blue) molar equivalents of TRX.

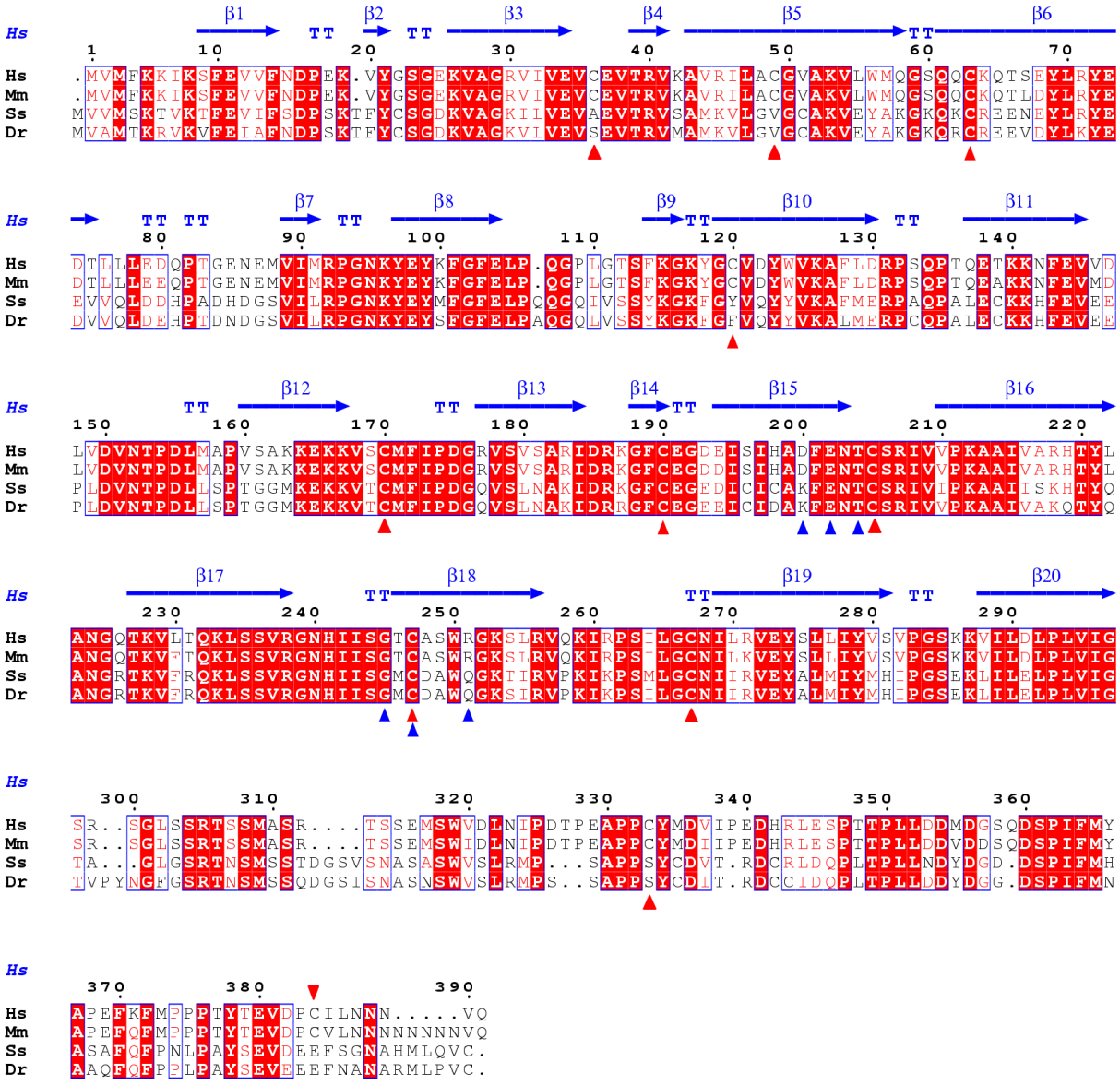

Supplementary Figure S11 | Alignment of TXNIP and homologous proteins from different species. The secondary structure of human TXNIP is shown above the alignments and the numbers are relative to this sequence. The red arrowheads indicate cysteine residues in TXNIP. Cys63, Cys170, Cys190, Cys205, Cys247, and Cys267 are strictly conserved, but Cys36, Cys49, Cys120, Cys333, and Cys384 are not. The blue arrowheads indicate residues that are critical for the interaction of TXNIP with TRX. Strictly conserved residues are highlighted in red (with white text). The biological sources and accession codes for the

sequences are as follows: Hs, *Homo sapiens* (gi:171184421); Mm, *Mus musculus* (gi:254553444); Ss, *Salmo salar* (gi:223647818); and Dr, *Danio rerio* (gi:41056117). Sequence alignments were assembled using CLUSTALW software and were visualized using ESPript software (both accessible via the ExPASy Proteomics Server: http://au.expasy.org/).

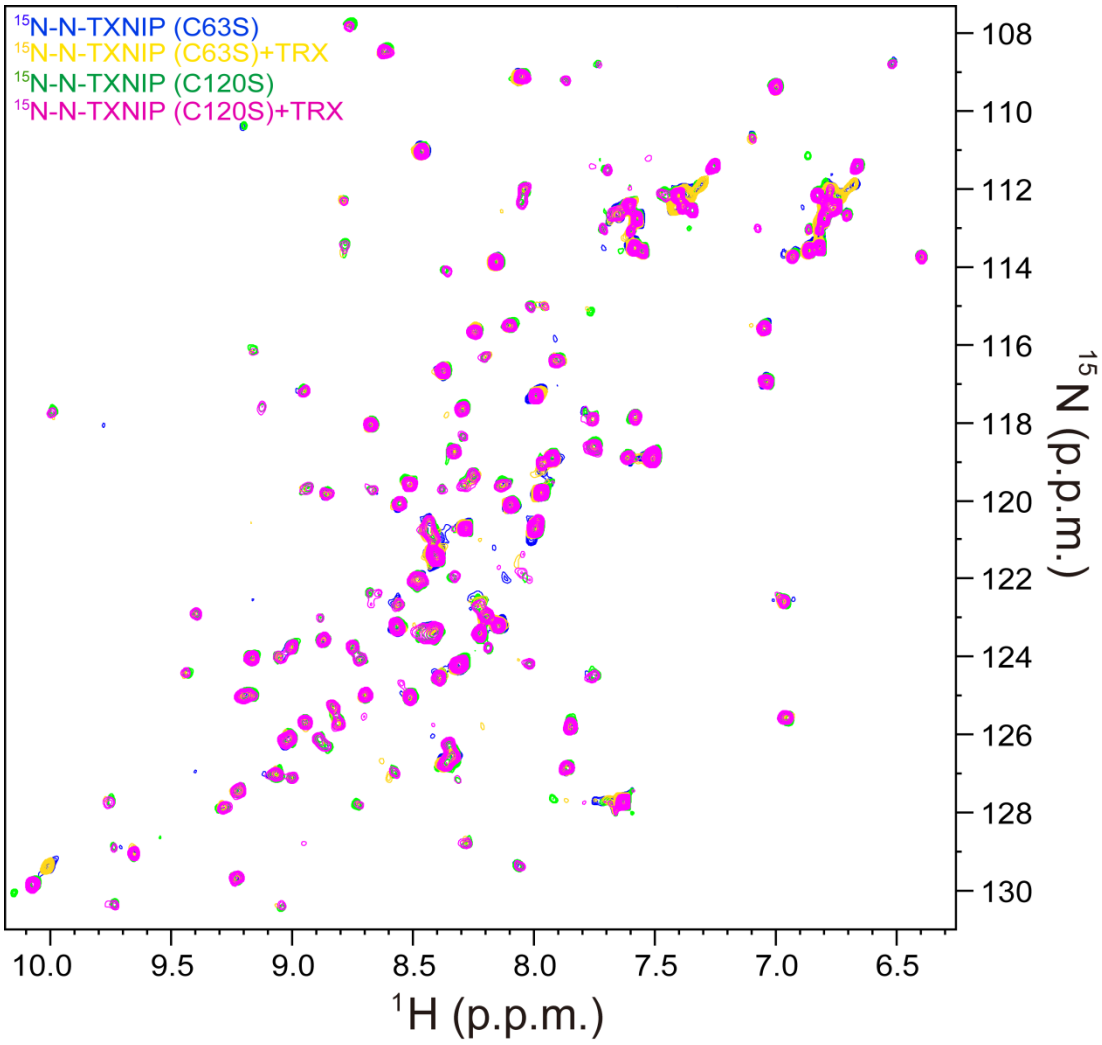

Supplementary Figure S12 | TRX interacts with a disulfide bond involving TXNIP Cys63. The results of ^{1}H-^{15}N HSQC NMR experiments performed using ^{15}N-labeled N-TXNIP mutants and TRX. Compared with the spectra of N-TXNIP(C63S) (blue) and N-TXNIP(C120S) (green) alone, there were no substantial chemical shifts when TRX was added to the C63S (yellow) or C120S (magenta) mutant.

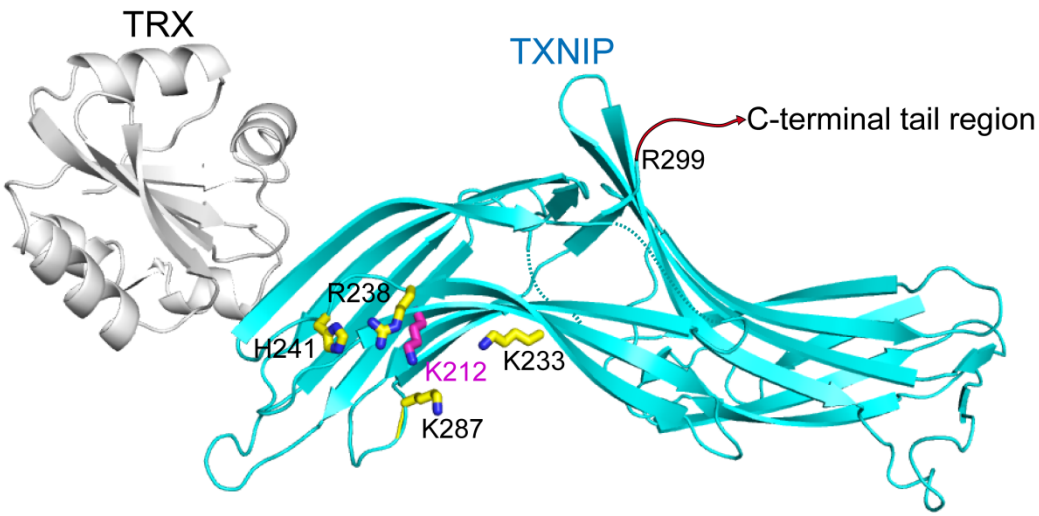

Supplementary Figure S13 | Location of the ubiquitinated residue Lys212 in the TXNIP structure complexed with TRX. The Lys2l2 residue is located in the highly basic C-terminal region, which forms a deeply curved β-sandwich domain. Lys212 is depicted as a stick with magenta carbon atoms. The residues with positive electrostatic potential in C-TXNIP are depicted as sticks with yellow carbon atoms. The C-terminal tail region beyond amino acid position R299 of TXNIP is indicated by a red arrow.

Supplementary Table S1 | Proteins identified in the 150 kDa protein band detected by SDS-PAGE.

Protein	Protein probability	Percent coverage	No. unique peps[a]	Tot. indep. spectra[b]	Description	Gene name	Subcellular location
TXNIP	1	56	33	77	TXNIP		
O95347	1	22.7	25	25	Structural maintenance of chromosomes protein 2	SMC2	Nucleus
Q08211	1	14.9	20	20	ATP-dependent RNA helicase A	DHX9	Nucleus
E5KNY5	1	13.3	19	19	Leucine-rich PPR-motif containing	LRPPRC	
P41252	1	15.8	19	19	Isoleucyl-tRNA synthetase, cytoplasmic	IARS	Cytoplasm
P53621	1	15.9	18	18	Coatomer subunit alpha	COPA	Cytoplasm
E7EMV2	1	20.5	13	13	Uncharacterized protein	NEFM	
F5H5D3	1	26.9	11	12	Uncharacterized protein	TUBA1C	
Q9UQE7	1	12.9	12	12	Structural maintenance of chromosomes protein 3	SMC3	Nucleus
A8K5I0	1	24.3	10	11	Heat shock 70 kDa protein 1A	HSPA1A	
E7EW20	1	9.3	10	10	Uncharacterized protein	MYO6	

[a]The number of unique peptides.

[b]The number of total independent spectra.

Supplementary Table S2 | Proteins identified in the 70 kDa protein band detected by SDS-PAGE.

Protein	Protein probability	Percent coverage	No. unique peps[a]	Tot. indep. spectra[b]	Description	Gene name	Subcellular location
A8K5I0	1	57.3	47	92	Heat shock 70 kDa protein 1A	HSPA1	
P11142	1	63.5	57	83	Heat shock cognate 71 kDa protein	HSPA8	Cytoplasm
TXNIP	1	55.5	54	80	TXNIP		
B7Z4V2	1	49.2	58	70	Uncharacterized protein	HSPA9	
P11021	1	42.4	28	29	78 kDa glucose-regulated protein	HSPA5	Endoplasmic reticulum lumen
P17066	1	40.3	29	29	Heat shock 70 kDa protein 6	HSPA6	
E7EQV3	1	26.2	20	20	Uncharacterized protein	PABPC1	
P12956	1	28.2	20	20	X-ray repair cross-complementing protein 6	XRCC6	Nucleus
Q15046	1	21.3	17	17	Lysyl-tRNA synthetase	KARS	Cytoplasm
Q9NZI8	1	30.5	17	17	Insulin-like growth factor 2 mRNA-binding protein 1	IGF2BP1	Nucleus
P04843	1	27.8	16	16	Dolichyl-diphosphooligosaccharide-protein glycosyltransferase subunit 1	RPN1	Endoplasmic reticulum membrane
P54136	1	23.8	14	14	Arginyl-tRNA synthetase, cytoplasmic	RARS	Cytoplasm
F5H897	1	21.8	13	13	Uncharacterized protein	TRAP1	
P07237	1	20.9	10	10	Protein disulfide-isomerase	P4HB	Endoplasmic reticulum lumen

[a]The number of unique peptides.

[b]The number of total independent spectra.

Supplementary Table S3 | Disulfide bonds and free cysteines identified by mass spectrometry.

		The number of spectra	
		~60 kDa	**~32 kDa**
Disulfide bonds*	C63 ─ C190	1	93
	C63 ─ C247	5	3
	C63 ─ C63	1	1
	C190 ─ C247	1	3
	C247 ─ C247	1	2
	Total	9	102
Free cysteines	C63	4	5
	C190	0	42
	C247	2	5
	Total	6	52

*Dbond score > 20.